

# Processing of medical images using real-time optical Fourier processing

Appaji Panchangam, K. V. L. N. Sastry, and D. V. G. L. N. Rao<sup>a)</sup>  
*Department of Physics, University of Massachusetts, Boston, Massachusetts 02125*

B. S. DeCristofano, B. R. Kimball, and M. Nakashima  
*U.S.S. Army Natick Research, Development and Engineering Center, Natick, Massachusetts 01760*

(Received 10 August 2000; accepted for publication 3 October 2000)

Optical image processing techniques are inherently fast in view of parallel processing. A self-adaptive optical Fourier processing system using photoinduced dichroism in a bacteriorhodopsin film was experimentally demonstrated for medical image processing. Application of this powerful analog all-optical interactive technique for cancer diagnostics is illustrated with two mammograms and a Pap smear. Microcalcification clusters buried in surrounding tissue showed up clearly in the processed image. By playing with one knob, which rotates the analyzer in the optical system, either the microcalcification clusters or the surrounding dense tissue can be selectively displayed. Bacteriorhodopsin films are stable up to 140 °C and environmentally friendly. As no interference is involved in the experiments, vibration isolation and even a coherent light source are not required. It may be possible to develop a low-cost rugged battery operated portable signal-enhancing magnifier. © 2001 American Association of Physicists in Medicine. [DOI: 10.1118/1.1328079]

Key words: bacteriorhodopsin, Photoinduced anisotropy, optical Fourier processing, self-adaptive image processing, mammograms

## I. INTRODUCTION

The incidence of breast cancer and its devastating effects in the United States is well documented<sup>1</sup> and the incidence rates are still high.<sup>2</sup> Early detection of cancer is extremely important for successful treatment. Computer aided diagnosis and digital image processing techniques have been widely investigated to improve the sensitivity of radiography and to improve objectivity of clinical cancer diagnosis.<sup>3-6</sup> However, digital radiographs contain large amounts of information in digital format. The best digitizers available digitize a radiograph to a 4 k×6 k-14 bit format.<sup>7-9</sup> They may not be able to preserve the contrast of the original analog image due to the errors in sampling.<sup>10</sup> Also digital computers manipulate data in series. Even though excellent algorithms can be designed to process the data, they are still time consuming and expensive. Hence these techniques are limited to elite academic and research institutions. Parallel and analog optical image processing techniques are well suited to improve the speed and reduce the cost. Optical processing techniques are widely recognized for their inherent advantages for real time image processing.<sup>11</sup>

In any given image all points (or pixels) in the two-dimensional plane of the image can be processed at the same time. Due to this inherent advantage of parallel processing, optical techniques (e.g., optical Fourier transform using a simple lens) are inherently fast. Optical image processors can be assembled with low-cost components like lenses, polarizers, mirrors and commercially available charge-coupled device (CCD) camcorders. Once assembled these devices require no or low maintenance. However conventional optical Fourier filtering techniques suffer from one serious disadvantage. A convex (positive) lens is used to obtain the Fourier

transform of the object at the focus (Fourier plane). Low frequencies (spatial) occur at the center with high intensity and high (spatial) frequencies are at the edges with low intensity. Conventional filtering techniques use masking. A small opaque mask placed at the center blocks low frequencies. High frequencies occurring at the edges (low intensity) go through. This is usually done for achieving edge enhancement. Similarly one can block high frequencies at the edges corresponding to low intensity by placing a mask at the edges. A band of frequencies somewhere in the middle can be blocked by placing masks at appropriate places (bandpass filtering). When the same object is resized or a different object is used or a lens of different focal length is used, the mask has to be realigned for the same image processing function (say edge enhancement) because the entire scenario at the focal plane changes.

### A. Digital image processing

A common approach for medical image processing is to convolute the two-dimensional (2D) image with a filter function.<sup>10,12,13</sup> The spatial image to be processed is converted into a spatial frequency spectrum. This is done using a fast Fourier transform algorithm in digital computers.<sup>10</sup> This operation involves  $n \log_e(n)$  floating point operations to convert the  $n$  pixel digital image to its Fourier transform. This Fourier transform is then multiplied with a filter function (generated on a computer) designed to achieve the desired enhancement. This operation requires  $n$  floating-point multiplications. The filtered spectrum is converted back to a 2D image by taking the inverse fast Fourier transform. The schematic of the process is depicted in Fig. 1.

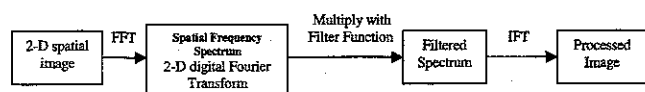


FIG. 1. Schematic of digital image processing. FFT, fast Fourier transform; and IFT, inverse Fourier transform.

## B. Hybrid digital-optical processing

More recently, optical techniques are being applied for image processing. Liu *et al.*<sup>14</sup> proposed a hybrid architecture for medical image processing. A positive lens is used to obtain optical Fourier transform of the object image at the first Fourier plane. The frequency spectrum obtained is written onto the write side of a spatial light modulator (SLM) placed at the focal plane of the lens. The optical pattern of desired bandpass filter generated by a computer is projected onto the other side of the SLM. The corresponding optical spectrum processed by the SLM is inverse Fourier transformed to obtain the final image, which can be stored or displayed on a CCD.

In both techniques, all digital and hybrid digital-optical, when the object is resized or changed, the situation at the Fourier plane changes entirely. So the computer has to locate the spatial frequency band to be filtered which changes with each object. Appropriate software has to be used for this function. This may involve complex algorithms and computer time.

In this paper we propose an analog all-optical self-adaptive real-time spatial filtering technique using bacteriorhodopsin film and analyzer combination as the main processing module.

## II. OPTICAL FOURIER PROCESSING

*Optical Fourier processing using bacteriorhodopsin.* Bacteriorhodopsin (bR) and photopolymers containing bR have shown great promise as candidate materials for applications in photonic technology.<sup>15,16</sup> Recently, we<sup>17-19</sup> demonstrated experimentally a self-adaptive optical Fourier-processing system, using photoinduced dichroic characteristics of a bR film with applications in noise reduction, edge enhancement, and bandpass filtering.

A schematic of the experimental technique is illustrated in Fig. 2 using 570 nm coherent light. We use lenses to obtain Fourier transform and inverse Fourier transforms. Optical filtering is also a simple analog process performed by the bR-analyzer combination. The property of polarization rotation depending on the image bearing beam intensity is used to encode the frequencies of the Fourier spectrum with a range of polarization information. The analyzer selectively blocks

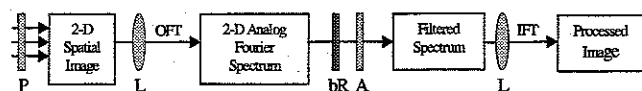


FIG. 2. Schematic of experimental arrangement for all-optical Fourier processing. P, polarizer; OFT, optical Fourier transform; L, lens; bR, bacteriorhodopsin film; A, analyzer; and IFT, inverse Fourier transform. bR-analyzer combination acts as self-adaptive spatial filter.

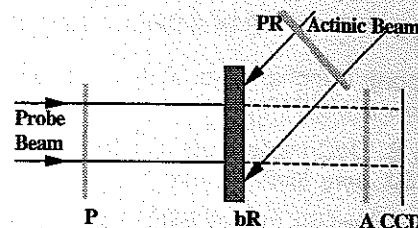


FIG. 3. Schematic of experimental arrangement for measuring photoinduced polarization rotation. Both actinic and probe beams are derived from Ar-Kr laser at 570 nm. P, polarizer; bR, bacteriorhodopsin; PR, polarization rotator; and A, analyzer. Actinic beam polarized at 45° with respect to the probe beam polarization.

the frequencies whose polarization vector is different from its optic axis. Thus we filter spatial frequencies by rotating the analyzer. We can scan through the entire frequency spectrum just by rotating the analyzer knob. The frequency spectrum filtered by the analyzer is converted to spatial information by inverse Fourier transforming with another Fourier lens.

## III. EXPERIMENTAL RESULTS

The experimental arrangement for measuring photoinduced angular rotation of the probe beam polarization is shown in Fig. 3. The polarization rotation of a weak probe beam as a function of actinic beam intensity is given in Fig. 4. Maximum rotation is observed at actinic intensity of 10 mW/cm<sup>2</sup>. Keeping the actinic beam at 10 mW/cm<sup>2</sup> we gradually increase the intensity of the probe beam. Figure 5 shows the experimental data. The system is highly sensitive to changes in probe intensity. The effect of increasing the probe intensity is to decrease the degree of polarization rotation of probe beam because high probe intensities reduce the anisotropy of bR film. With intensities of the order of ~10 mW/cm<sup>2</sup> for probe beam the angular rotation is nearly zero. The fact that increasing the probe beam's intensity reduces

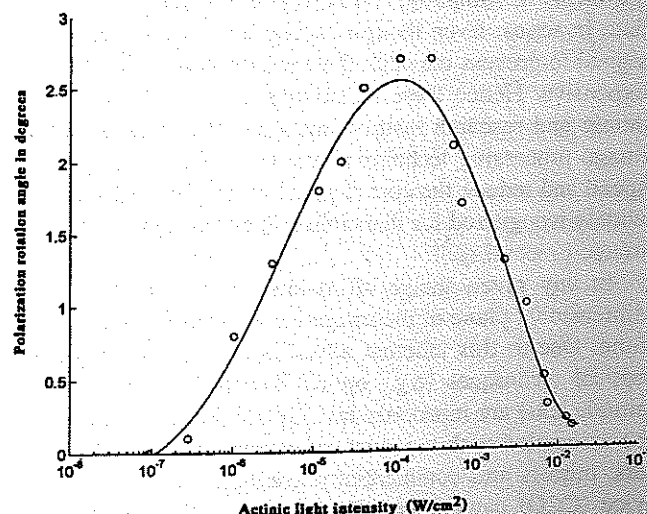


FIG. 4. Dependence of photoinduced polarization rotation on actinic beam intensity with constant probe beam intensity. The solid curve is intended solely as a visual aid.

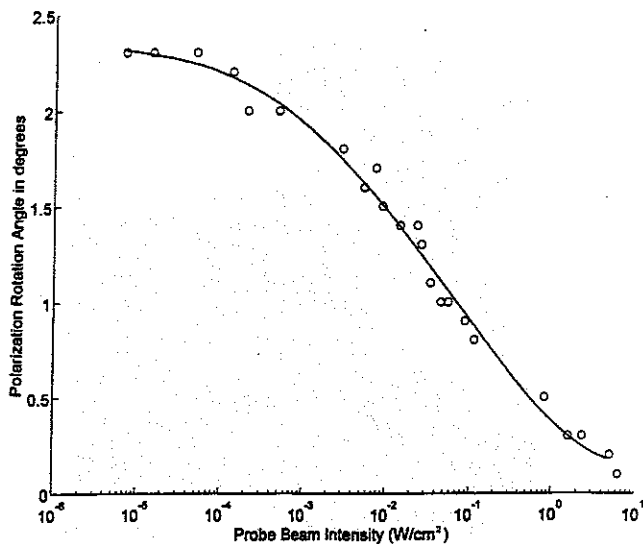


FIG. 5. Dependence of photoinduced polarization rotation on probe beam intensity with constant actinic beam intensity of  $10 \text{ mW/cm}^2$ . The solid curve is intended solely as a visual aid.

the angle of rotation of probe beam polarization passing through the bR film illuminated by the actinic light was exploited for optical Fourier processing.

Figure 6 shows the experimental setup used for optical Fourier processing using photoinduced dichroism in the bR film. Lens L1 forms the Fourier transform of the object information (O) at the bR film, and lens L2 forms the inverse Fourier transform at the CCD plane to yield the processed image. The actinic beam illuminates the bR film uniformly. The wild type bR film used in the experiment is purchased from Wacker Chemical Inc. (USA). It has a thickness of  $35 \mu\text{m}$ , and is sandwiched between glass plates. Initially with no actinic beam present, the polarizer (P) and the analyzer (A) are crossed with respect to each other, so that no light from the probe beam reaches the CCD. The self-adaptive image processing is explained as follows: In the experiment a vertically polarized laser beam illuminates the object (mammogram) uniformly. The light transmitted by the object has only one polarization (vertical). The positive lens forms the Fourier transform of the object on the bR plane. It has an intensity distribution with high intensities for low (spatial) frequency components near the center and low intensities for high frequency components on the edge. It may be observed from Fig. 5 that (low intensity) high frequency components at the bR plane experience higher degrees of polarization

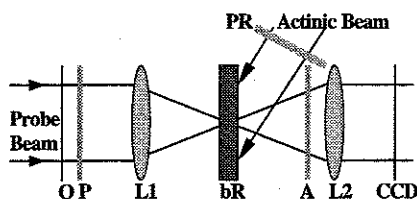


FIG. 6. Schematic experimental arrangement for optical Fourier processing. O, object; P, polarizer; L1, Fourier lens; PR, polarization rotator; L2, inverse Fourier lens; A, analyzer; and bR, bacteriorhodopsin.

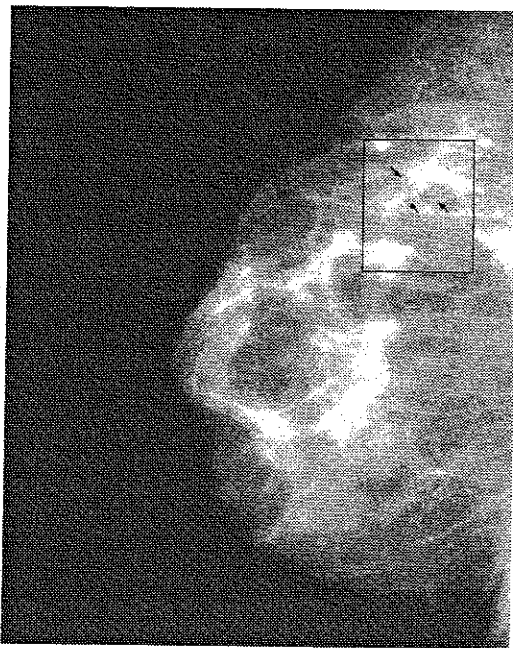
rotation than (high intensity) zero and low frequency components near the center (of the focal plane). The input object information has a single linear polarization (vertical). After its passage through the bR (under actinic light illumination) it has acquired a range of polarizations of different orientations. A band of spatial frequencies corresponding to a narrow region of intensity in the Fourier plane acquire a specific polarization. Thus there is a correspondence between spatial frequency—intensity—polarization rotation. In other words each spatial frequency band is encoded with a unique polarization. The Fourier processing is accomplished through the analyzer, which blocks specific polarization components in turn blocking the corresponding spatial frequencies. When the analyzer is at right angles to the input beam polarization, zero and low frequency components, which experience almost no polarization rotation because of their high intensities, are blocked by the analyzer. However, the high frequency components that correspond to the edges of the object experience polarization rotation, and are thus transmitted through the analyzer to appear at the CCD camera to yield edge enhancement. Rotation of the analyzer serves as a variable spatial filter for Fourier processing.

When the same object is resized or a different object is used (or the Fourier lens is changed), there is no need for any realignment of the system. Let us say we are interested in looking at microcalcifications in the mammogram (edge enhancement). The system is set for this application by crossing the analyzer and polarizer to block low spatial frequencies corresponding to dense tissue. When the object is resized or a different mammogram is used, or a lens of different focal length is used the scenario at the Fourier plane entirely changes. But the system self-adapts to the new situation and will still be able to perform the functions of edge enhancement and display microcalcifications. This is the unique advantage of the technique. In all other image processing techniques the filters have to be changed for the same application (edge enhancement and display microcalcifications) whenever the object is resized or changed.

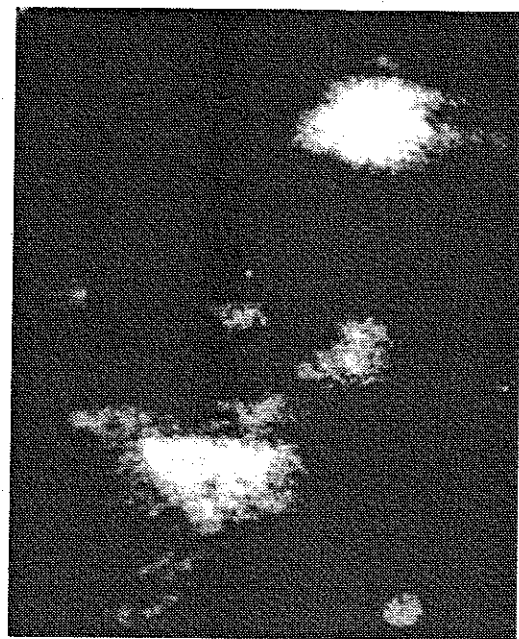
Experiments are conducted on mammograms and pap smears. We used two mammograms—one is a real clinical mammogram and the other is a photographed slide of a scanned picture from a printed paper. In the second case there is a lot of detail lost due to printing, scanning, and photographing the scanned picture to make a slide.

#### A. With a clinical mammogram

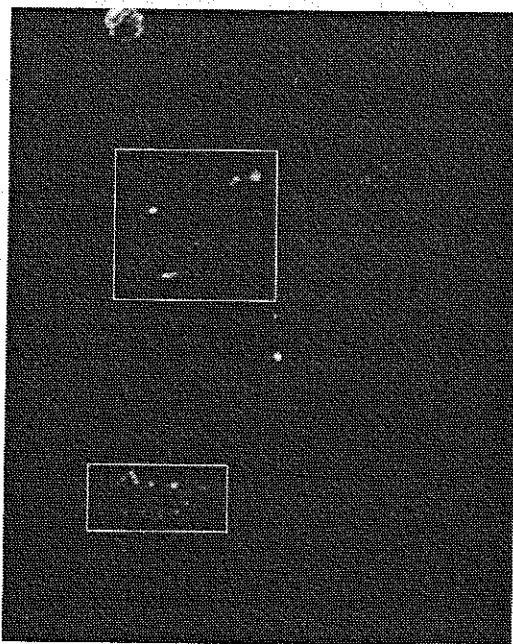
Our results on the clinical mammogram are illustrated in Fig. 7. The experimental arrangement used is the same as shown in Fig. 6. Figure 7(a) shows the unprocessed region of interest (ROI) of the mammogram. The arrows point out the site of probable microcalcification clusters. Initially the polarizer and analyzer are crossed and no light reaches the CCD. Figure 7(b) shows the image of the object when the actinic beam is turned on. The processed image clearly shows the microcalcifications not visible in the original mammogram. In this case the (high intensity) low spatial frequency components of the Fourier transform are filtered



(a)



(c)



(b)

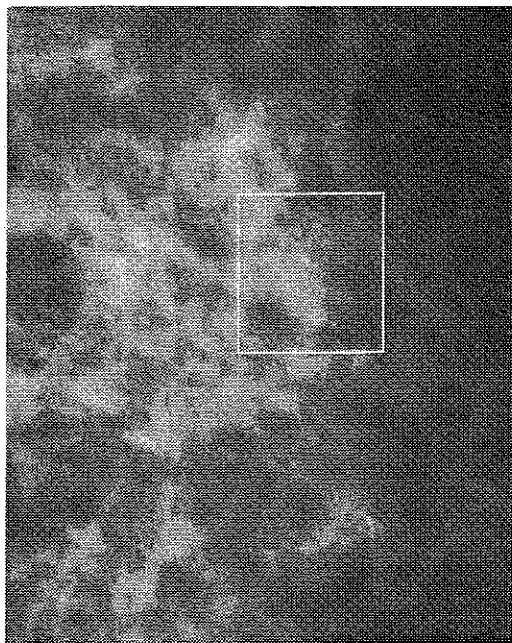
FIG. 7. (a) Region of interest of an unprocessed mammogram. (b) Microcalcifications are shown in the boxes (polarizer, analyzer crossed). (c) Surrounding dense tissue (analyzer rotated by  $\sim 1^\circ$ ).

out. The (low intensity) high frequency components undergo polarization rotation and are selectively enhanced. This occurs when the analyzer is set near the crossed position relative to the polarizer. We see by slightly rotating the analyzer by a few degrees that it is possible to selectively enhance the intensity of the low frequency components. The high frequency components are filtered out for this orientation. This is shown in the Fig. 7(c). Here we see the surrounding dense tissue, which corresponds to the low frequency components in the optical Fourier transform. These pictures illustrate that

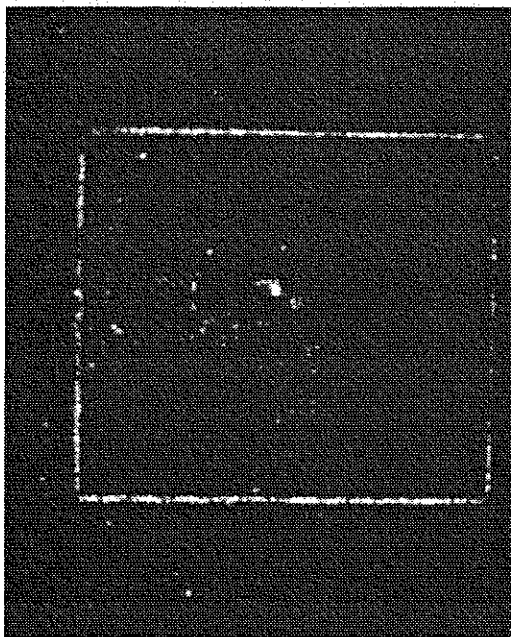
by slightly rotating the analyzer we can selectively enhance different frequencies in the Fourier transform.

#### B. With scanned picture of a mammogram

We used a slide made out of a scanned picture of a printed mammogram taken from DeVore *et al.*'s article.<sup>20</sup> Figure 8(a) shows a picture of unprocessed image. The ROI is the box, which was originally there in the picture from which we scanned our object. Figure 8(b) shows the microcalcifica-



(a)



(b)

FIG. 8. (a) Unprocessed picture of a mammogram. (b) Microcalcifications. The edges of the box from the original picture can be seen as they correspond to similar frequencies in Fourier spectrum.

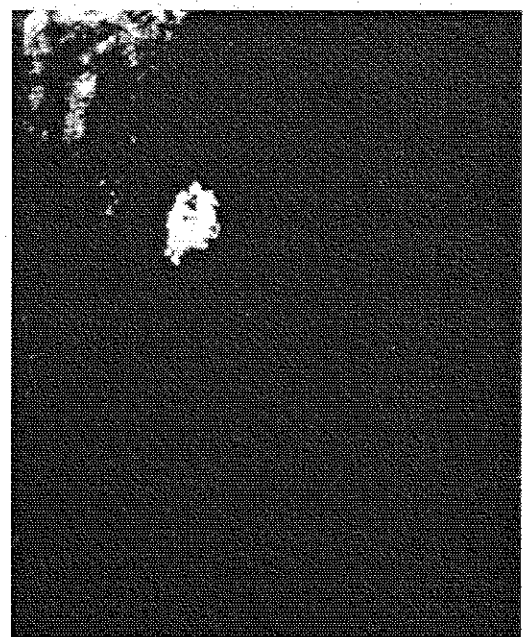
tions identified. The edges of the box are also visible as they correspond to similar frequencies in the Fourier spectrum.

### C. With Pap smears

Our technique is also applicable for studying Pap smears. Figure 9(a) shows a section of a Pap smear. Here we are using a reversed image of a Pap smear. The bright spots represent the nuclei. Both normal and abnormal nuclei are



(a)



(b)

FIG. 9. (a) Unprocessed image of a Pap smear slide. (b) Abnormal cells. Normal cells are filtered out.

visible in this picture. In Fig. 9(b), the normal nuclei are filtered out retaining only the abnormal nuclei (large cluster). This is achieved by selectively filtering out high frequency components in the Fourier transform (by rotating the analyzer).

### IV. CONCLUSION

We demonstrated a self-adaptive real-time image processing technique for processing medical images. The experi-

mental setup is flexible and can be adapted to handle digital images as well. As no interference is involved, vibration isolation and a coherent source are not required. The technique is versatile and can be used for identifying bacteria in cell cultures. It is possible to build a field deployable, efficient, and environmentally friendly optical Fourier image processor that works in real time. With the increasing availability of low-cost optics a handy cam size product can be built.

## ACKNOWLEDGMENTS

The real clinical mammogram was obtained from the Radiology Department, U. Mass. Medical School, Worcester, MA. We thank Dr. Carl D'orsis and Professor Andrew Karelis.

<sup>1</sup>C. C. Boring, T. S. Squires, and T. Tong, "Cancer statistics 1991," *CA-A Cancer Journal for clinicians* 41(1), 19-51 (1991).

<sup>2</sup>*Cancer Facts & Figures—1997* (American Cancer Society, Atlanta, 1997).

<sup>3</sup>J. Dengler, S. Behrens, and J. F. Desaga, "Segmentation of microcalcifications in mammograms," *IEEE Med. Imaging* 12(4), 634-642 (1993).

<sup>4</sup>H. Schiabel, F. L. S. Nunes, P. M. Azevedo Marques, and A. F. Frere, "A computerized scheme for detection of clusters of microcalcifications by mammogram image processing," *World Congress on Medical Physics and Biomedical Engineering (NICE 97)* (unpublished), pp. 14-19.

<sup>5</sup>Y. Wu, K. Doi, M. L. Giger, and R. M. Nishikawa, "Computerized detection of clustered microcalcifications in digital mammograms: Application of artificial neural networks," *Med. Phys.* 19, 555-560 (1992).

<sup>6</sup>F. F. Yin, M. L. Giger, K. Doi, C. J. VyBorny, and R. A. Schemidt, "Computerized detection of masses in digital mammograms: Automated alignment of breast images and its effect on bilateral-subtraction technique," *Med. Phys.* 21, 445-452 (1994).

<sup>7</sup>A. Visweswaran, H. Liu, L. L. Fajardo, and G. A. DeAngelis, "Compari-

son of contrast detail curves of full field of view digital and screen film phantom breast images," *Front. Bio Med. Sci.* 1, 5-7 (1996).

<sup>8</sup>L. Cheng and R. Coe, "Full-field single-exposure digital mammography," *Med. Electron.* 155, 50-56 (1995).

<sup>9</sup>H. Liu, L. L. Fajardo, R. Baxter, J. Chen, J. McAdoo, G. Halama, and A. Jalink, "Full-size, high spatial resolution digital mammography using CCD scanning technique," in *Digital Mammography '96*, edited by K. Doi, M. L. Giger, R. M. Nishikawa, and R. A. Schmidt (Elsevier Science, Amsterdam, 1996), pp. 145-150.

<sup>10</sup>R. C. Gonzalez and P. Wintz, *Digital Image Processing*, 2nd Ed. (Addison-Wesley, Reading, MA, 1987).

<sup>11</sup>B. Javidi and J. L. Horner, in *Real-time Optical Information Processing* (Academic, Boston, MA, 1994).

<sup>12</sup>E. H. Linfoot, *Fourier Methods in Optical Image Evaluation* (Focal, London, 1964).

<sup>13</sup>E. G. Steward, *Fourier Optics—an Introduction* (Horwood, Chichester, 1987), Chap. 5.

<sup>14</sup>H. Liu, J. Xu, L. L. Fajardo, S. Yin, and F. T. S. Yu, "Optical processing architecture and its potential application for digital and analog radiography," *Med. Phys.* 26, 648-652 (1999).

<sup>15</sup>R. R. Birge, "Protein-based computers," *Sci. Am.* 90 (March 1995).

<sup>16</sup>D. Oesterhelt, C. Brauchle, and N. Hampp, "Bacteriorhodopsin: A biological material for information processing," *Q. Rev. Biophys.* 24, 425 (1991).

<sup>17</sup>J. Joseph, F. J. Aranda, D. V. G. L. N. Rao, J. A. Akkara, and M. Nakashima, "Optical Fourier processing using photoinduced dichroism in a bacteriorhodopsin film," *Opt. Lett.* 21, 1499-1501 (1996).

<sup>18</sup>J. Joseph, F. J. Aranda, D. V. G. L. N. Rao, and B. S. DeCristofano, "Optical computing and information processing with a protein complex," *Opt. Mem. Neural Networks* 6, 275-285 (1997).

<sup>19</sup>J. Joseph, F. J. Aranda, D. V. G. L. N. Rao, and B. S. DeCristofano, "Optical implementation of the wavelet transform by using a bacteriorhodopsin film as an optically addressed spatial light Modulator" 73, 1484-1486 (1998).

<sup>20</sup>R. A. Devore, B. Lucier, and Z. Yang, "Feature extraction in digital mammography," *WAVELETS in Medicine and Biology*, edited by A. Aldroubi and M. Unser (CRC, Boca Raton, FL, 1996), pp. 158.